Journal of Hazardous Materials 203–204 (2012) 86–92

Contents lists available at SciVerse ScienceDirect

Journal of Hazardous Materials

journal homepage: www.elsevier.com/locate/jhazmat

Nitrate removal from aqueous solution by *Arundo donax* L. reed based anion exchange resin

Xing Xu [a], Baoyu Gao [a,*], Yaqing Zhao [a], Suhong Chen [a], Xin Tan [a], Qinyan Yue [a], Jianya Lin [b], Yan Wang [a]

[a] Key Laboratory of Water Pollution Control and Recycling (Shandong), School of Environmental Science and Engineering, Shandong University, Jinan 250100, PR China
[b] State Key Laboratory of Microbial Technology, School of Life Science and Engineering, Shandong University, Jinan 250100, PR China

ARTICLE INFO

Article history:
Received 26 September 2011
Received in revised form
25 November 2011
Accepted 25 November 2011
Available online 8 December 2011

Keywords:
Arundo donax L. reed
Resin
Nitrate
Raman spectra
Competitive adsorption

ABSTRACT

Arundo donax L. reed based anion exchange resin (ALR-AE resin) was prepared by the amination reaction for the adsorption of nitrate from aqueous solution. The physicochemical properties of the ALR-AE resin as well as its adsorption properties for nitrate were measured. Results indicated that large amounts of amine groups have been grafted onto the structure of the resin. The FTIR and Raman spectra validated the ion exchange mechanism for nitrate adsorption by ALR-AE resin. The adsorption data showed an exothermic nature for the adsorption of nitrate by ALR-AE resin, and the equilibrium time for the adsorption process was about 10 min. The maximum adsorption capacity (Q_{max}) for nitrate was 44.61 mg/g. The saturated adsorption capacity of ALR-AE resin in column was about 38.9 mg/g, which accounted for about 87.2% of the resin's Q_{max}. The preferential adsorption capacity of the ALR-AE resin followed the order as: $SO_4^{2-} > NO_3^- \approx PO_4^{3-} > NO_2^-$. In addition, the utilization of the resin in actual water samples indicated that the ALR-AE resin could be used for the treatment of many ionic polluted wastewaters.

1. Introduction

In the last decade, a great attention has been focused on the search of new non-food crops with perspective for industrial utilization in China [1,2]. A widely distributed naturally growing hydrophyte, *Arundo donax* L. reed, has been considered as one of the more potential crops, ascribed to its easy adaptability to different ecological conditions [3,4], high biomass productivity and ability to intensive cultivation [5,6]. In addition to this, the appropriate chemical composition in *A. donax* L. reed with 21.1% of lignin, 31.1% of cellulose (as α-cellulose) and 30.3% of hemicelluloses makes it very attractive for pulp and paper industry by using as an alternative source of fibers [7–11]. Recent years, a series of studies on applicability of *A. donax* L. reed have been enhanced, and some modification methods have showed a potential application to produce high quality and ecologically friendly adsorbents [12–18].

The adsorbents prepared from *A. donax* L. reed included *A. donax* L. reed based active carbon (ALR-AC) and *A. donax* L. reed based resin (ALR-AE resin). A series of ALR-AC were prepared by the carbonization and activation process (in acidic/alkaline condition) at high temperature [13–15]. These ALR-AC showed high adsorption capacities for some organic contaminants, but were limited in the use of ionic polluted wastewaters. In contrast to the ALR-AC, ALR-AE resin broadened its adaptability on the adsorption of ionic pollutants. The preparation of ALR-AE resin was based on the large amount of easily available hydroxyl groups existing in cellulose, hemicelluloses and lignin, which can easily actuate a series of cross-linking reactions, such as esterification, etherification and copolymerization [6,12].

Lake eutrophication has become a serious environmental problem, and nitrogen is generally considered to be a significant nutrient in water eutrophication [19,20]. The release of large amounts of nitrogen-bearing wastes to surface water can stimulate the organisms and algaes growths in most ecosystems, which in turn, have a harmful effect on fish and other aquatic life, resulting in deterioration of water quality [21]. So the removal of nitrogen from the aquatic environment is required. In this work, we use the hydrophyte based resin, ALR-AE resin as the adsorbent material to uptake the nitrate from the aqueous solution. The ALR-AE resin used in this work was prepared by the amination reaction. The physicochemical properties of the ALR-AE resin were measured, using the instruments such as elemental content analyzer, Raman spectrometer, microelectrophoresis apparatus and Fourier transform infrared spectroscopy (FT-IR) analyzer. The adsorption properties of the ALR-AE resin for nitrate were determined by the static and dynamic adsorption tests. The competitive adsorption property (NO_3^-, SO_4^{2-}, PO_4^{3-} and NO_2^-) was discussed, and in addition to this, some actual water samples were selected to evaluate the applicability of ALR-AE resin in practical utilization.

* Corresponding author. Tel.: +86 531 88364832; fax: +86 531 88364513.
E-mail addresses: bygao@sdu.edu.cn, baoyugao_sdu@yahoo.com.cn (B. Gao).

0304-3894/$ – see front matter © 2011 Elsevier B.V. All rights reserved.
doi:10.1016/j.jhazmat.2011.11.094

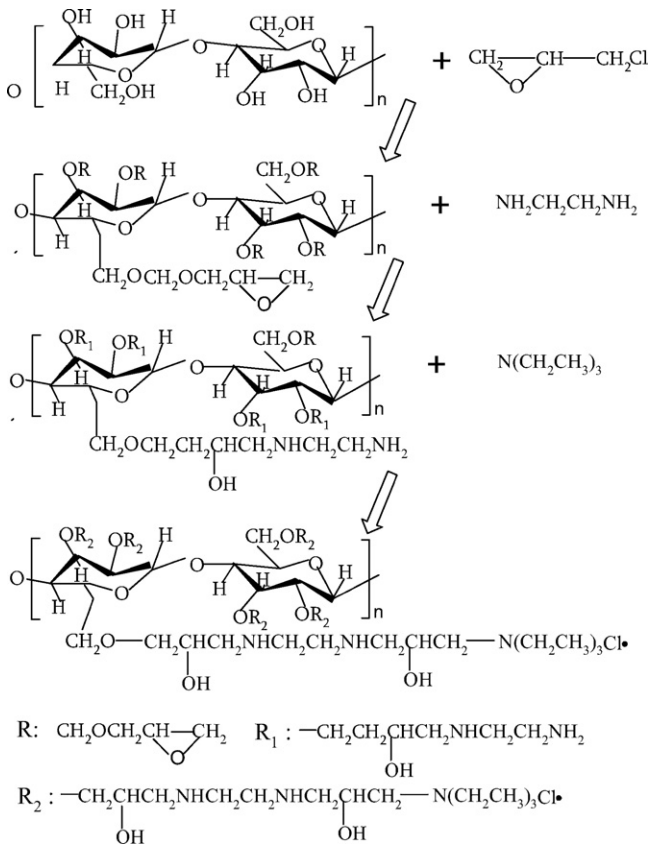

Fig. 1. Chain reaction between cellulose/hemicellulose chains and grafting chemical reagents.

2. Materials and methods

2.1. Preparation

The raw *A. donax* L. reed was obtained from Nansi Lake, Jinin, China. The raw reed was smashed into fragments with lengths of 0.2–1.0 cm, and thereafter the smashed *A. donax* L. reed was washed with water and then dried at 105 °C for 24 h. The procedures for the preparation of ALR-AE resin included three stages following as [12,22]:

(1) Stage 1. Ten gram of *A. donax* L. reed was reacted with 10 mL of epichlorohydrin and 6 mL of N,N-dimethylformamide in a three-neck round bottom flask, and the reactants were stirred at 85 °C for 60 min.
(2) Stage 2. Three milliliter of diethylenetriamine was added and the mixture was stirred for 5 min at 85 °C, followed by adding 9 mL of triethylamine for grafting and stirring for 120 min at 85 °C.
(3) The product was washed with 250 mL of distilled water to remove the residual chemicals, dried at 60 °C for 12 h and then used in the following characteristics and adsorption tests.

The scheme of the reaction was shown in Fig. 1, which has been reported in our previous work [22]. The preparation of ALR-AE resin was the chain reactions between cellulose/hemicellulose chain and side chains of different grafting chemical reagents. N,N-dimethylformamide was used as an organic medium which enhanced the susceptibility of the epoxide ring in epichlorohydrin. Ethylenediamine could be used as a crosslinking agent for some synthesis reactions between epichlorohydrin and amine.

2.2. Analytical methods on characteristics of the ALR-AE resin

In this work, the physicochemical properties of the ALR-AE resin were determined by using the elemental content analyzer, microelectrophoresis apparatus, Raman spectrometer and FT-IR analyzer. The grafted amine groups on ALR-AE resin were evaluated by comparing the nitrogen contents between ALR-AE resin and raw *A. donax* L. reed, which were measured by the element analyzer (Elementar Vario EL III, Germany). A microelectrophoresis apparatus (JS94H, Shanghai Zhongchen Digital Technical Apparatus Co. Ltd., China) was used to determine the zeta potentials of ALR-AE resin and raw *A. donax* L. reed. The samples were prepared in 25 mL of distilled water containing 0.1 g of ALR-AE resin/raw *A. donax* L. reed. In addition, the nitrate-loaded ALR-AE resin was prepared by comprising the suspensions with 0.1 g of the resin and 100 mg/L nitrate.

The functional groups presenting in ALR-AE resin and raw *A. donax* L. reed were investigated by using the FTIR technique (Perkin-Elmer "Spectrum BX" spectrometer). The spectrum was scanned from 400 to 4000 cm^{-1}. In the Raman analysis, 0.1 g ALR-AE resin was placed in 50 mL of nitrate solution (0.5 mol/L). The wet solid samples and nitrate solution (1 mol/L) were analyzed by Raman spectroscopy (Nicolet Almega XR Dispersive Raman, Thermo Electron Corporation, USA). The laser wavelength used in Raman measurement was 1050 nm.

2.3. Adsorption tests

2.3.1. Static sorption tests

The static sorption tests were carried out by using a sample containing 0.1 g of ALR-AE resin and 50 mL of nitrate solution in 250 mL flasks and shaking on a horizontal shaker. In the contact time test, at specified time intervals of 1, 3, 5, 8, 10, 15, 20, 30, 45, 60, 80, 120 and 150, an aliquot of sample was taken and analyzed for the residual concentration of nitrate in the supernatant solution at different pH (2.0–12.0). The pH was adjusted using 1 mol/L of HCl and NaOH. In the batch equilibrium experiments, the sorption experiments were performed at various initial concentrations for 60 min at four temperatures (293, 303, 313 and 323 K). The concentration of the nitrate was measured using PCI-8 ion chromatograph (Qingdao Puren Instrument Co. Ltd.) and all the experiments were performed in duplicate and the average result was taken for calculation.

2.3.2. Dynamic (column) adsorption and competitive adsorption tests

Column studies (up flow mode) were conducted in organic-glass column with an internal diameter of 1.2 cm and 20 cm in length. The flow rate was constant with 5 mL/min and the concentration of nitrate solution was 100 mg/L. The packed ALR-AE resin in column was controlled with 0.5 g, 1.0 g and 2.0 g. The effluent solutions were collected, and every 10 mL was selected as a sample to determine the residue concentrations in the effluent solutions. The flow to the column was continued until the effluent concentration (C_t) approached the influent concentration (C_0), $C_t/C_0 = 0.98$.

The competitive adsorption showed the preferential adsorption properties of ALR-AE resin for various anions. Four coexisting anions (NO_3^-, SO_4^{2-}, PO_4^{3-} and NO_2^-) were selected and their concentrations were in range of 10–50 mg/L.

2.3.3. Utilization of ALR-AE resin in actual water samples

The applicability of ALR-AE resin in practical utilization was evaluated by using the resin in three actual water samples. These actual water samples were obtained from 1# Longhu Mountain reservior (Jinan, China), 2# effluent from the wastewater treatment plant (Guangda wastewater plant, Jinan, China) and 3# Yihe River (Linyi, China). Their water qualities are shown in Table 1.

Table 1
Water qualities of three actual water samples.

No.	Actual water samples	Water qualities
1#	Longhu mountain reservoir	pH: 8.3; NO_3^-: 4.49 mg/L; NO_2^-: 0.36 mg/L; PO_4^{3-}: 0.16 mg/L; SO_4^{2-}: 5 mg/L
2#	Effluent from the wastewater treatment plant	pH: 8.7; NO_3^-: 36.5 mg/L; NO_2^-: 11.32 mg/L; PO_4^{3-}: 6.96 mg/L; SO_4^{2-}: 75.7 mg/L
3#	Yihe river	pH: 8.1; NO_3^-: 21.5 mg/L; PO_4^{3-}: 3.3 mg/L; SO_4^{2-}: 54.6 mg/L; AsO_2^-: 1.24 mg/L

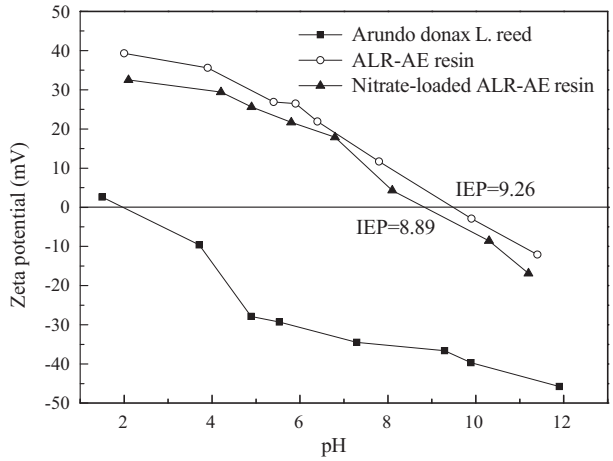

Fig. 2. Zeta potentials of *Arundo donax* L. reed, ALR-AE resin and nitrate-loaded ALR-AE resin as a function of pH (equilibrium pH).

Sulfate, phosphate, nitrite as well as nitrate were also detected by PCI-8 ion chromatograph (Qingdao Puren Instrument Co. Ltd.). The arsenic ions were detected by XGY-6060 atomic fluorescence spectrometry (Nanjing Xuhan Instrument Co. Ltd.).

3. Results and discussions

3.1. Characteristics of ALR-AE resin

3.1.1. Zeta potential analysis

The electrokinetic behavior of the samples in solution is one of the most important properties in characterization. Zeta potentials of raw *A. donax* L. reed, ALR-AE resin and nitrate-loaded ALR-AE resin as a function of pH were shown in Fig. 2. The zeta potentials of raw *A. donax* L. reed were in the range of +2.2 to −45.8 mV as the initial pH of the suspensions increases from 1.5 to 12.0. After the modification, the zeta potentials of ALR-AE resin increased significantly (+39.6 to −12.0 mV) in designed pH range; this illustrated an increased positive-charged functional groups on framework of ALR-AE resin. The decrease in zeta potentials of these samples as a function of pH could be attributed to the pH-dependent functional groups existing in raw *A. donax* L. reed and ALR-AE resin, such as hydroxyl and carboxyl groups. These groups would exhibit a greater negative charge as the pH increases and result in the decrease of the positive charge in these samples [23].

The isoelectric point (IEP) for ALR-AE resin was 9.26, whereas the IEP for nitrate-loaded ALR-AE resin was 8.89. The results showed that there was a slight shift in the IEP between the ALR-AE resin and nitrate-loaded ALR-AE resin. The decreased IEP in nitrate-loaded ALR-AE resin could be attributed to displacement of chloride ions by the adsorbed nitrate ions due to steric effects. Similar result was reported in the work of Yoon et al. for the sorption of perchlorate by resin and active carbon [24].

3.1.2. Elemental characteristics analysis

Table 2 shows the elemental changes between ALR-AE resin and raw *A. donax* L. reed. It was shown that the carbon content, hydrogen content and nitrogen content in raw *A. donax* L. reed were about 42.10%, 6.60% and 0.90%. After the cross-linking reaction, a significant increase in the nitrogen content (0.90–6.98%) was observed in the compositions of ALR-AE resin; this indicated that large amounts of amine groups have been grafted onto the structure of cellulose chains, resulting in the increase of nitrogen content in ALR-AE resin. This result was similar to the reported data in our previous work for the preparation of wheat straw, corn straw and cotton stalk based biosorbents [25–28].

Table 2
Elemental changes between ALR-AE resin and raw *Arundo donax* L. reed.

	N (%)	C (%)	H (%)
Raw *Arundo donax* L. reed	0.9	42.10	7.60
ALR-AE resin	6.98	41.55	8.22

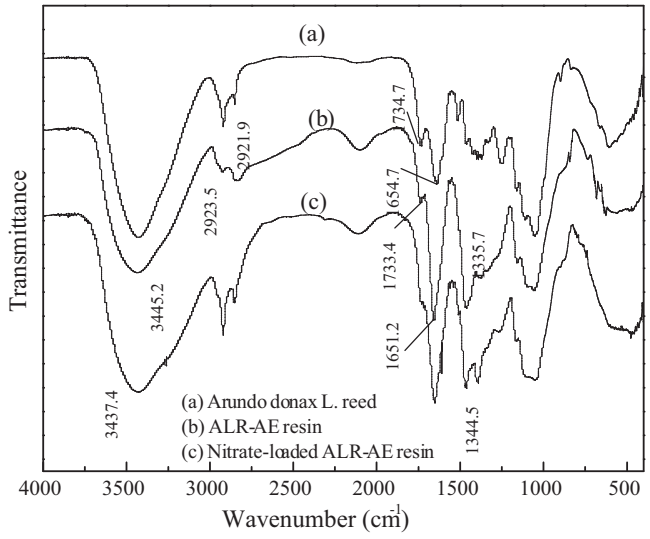

Fig. 3. FTIR spectra of raw *Arundo donax* L. reed, ALR-AE resin and nitrate-loaded ALR-AE resin samples.

3.1.3. FTIR spectra analysis

Fig. 3 shows the FTIR spectra of raw *A. donax* L. reed, ALR-AE resin and nitrate-loaded ALR-AE resin samples. The FTIR spectra analysis of these samples illustrated the change of functional groups.

In FTIR spectra of raw *A. donax* L. reed and ALR-AE resin, the band at 3300–3400 cm^{-1} was assigned to hydroxyl groups (–OH) of macromolecular association in cellulose, hemicellulose, pectin, etc. [29]. Aromatic cyclic groups were observed by the band intensity at 1654.7 (1651.2) cm^{-1}, and the band at 2923.5 (2921.9) cm^{-1} was associated with the special vibration of $-CH_2$. The band observed at 1734.7 (1733.4) cm^{-1} was assigned to the carboxyl group (–COO) stretching [29]. Appearance of new peak around 1335.7 cm^{-1} was assigned to C–N stretching vibration, which corresponded to the amine groups in the framework of ALR-AE resin [30]. The appearance of band at 734.4 cm^{-1} corresponded to the stretching vibration of the C–Cl bond, which was obtained from the grafted chemical reagent of epichlorohydrin.

After the adsorption of nitrate onto ALR-AE resin, the characteristic band C–N were shifted at the peak maximum (1335.7 → 1344.5 cm^{-1}). The special vibration C–Cl at 734.4 cm^{-1}

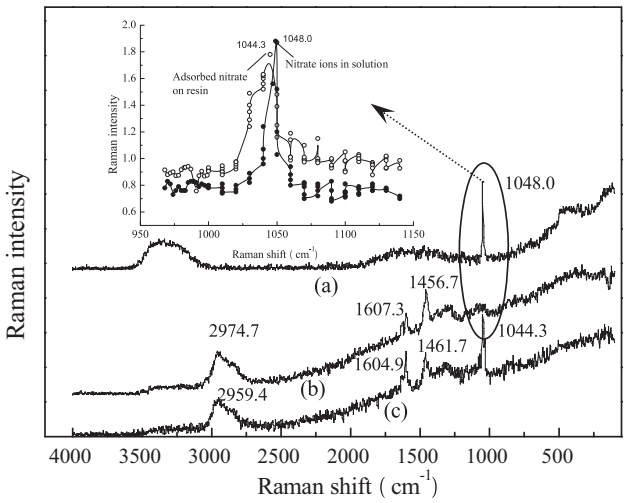

Fig. 4. Raman spectra of nitrate solution, ALR-AE resin and nitrate-loaded ALR-AE resin samples.

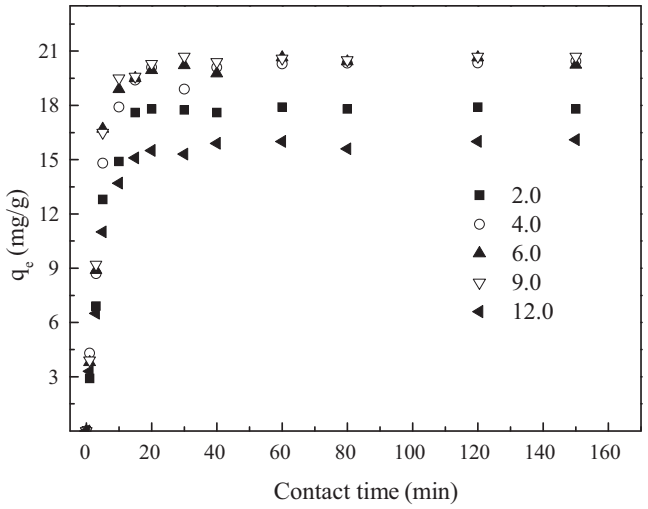

Fig. 5. Effect of contact time on the adsorption capacities for nitrate at different pH (nitrate concentration: 50 mg/L; ALR-AE resin dosage: 2 g/L).

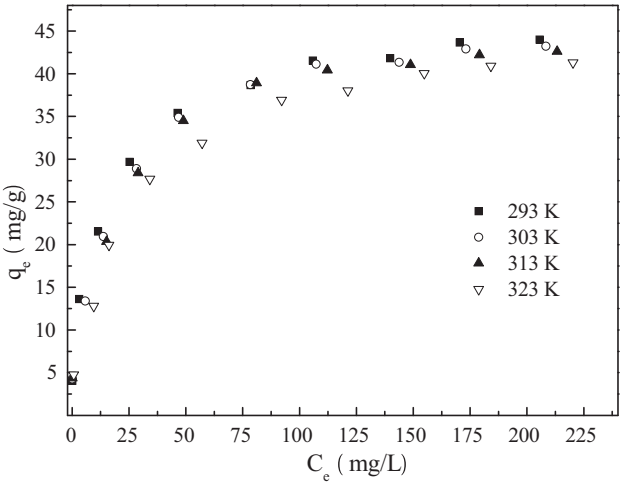

Fig. 6. Adsorption isotherm of ALR-AE resin for nitrate at different temperature (dosage of ALR-AE resin: 2 g/L).

disappeared in FTIR spectrum of nitrate-loaded ALR-AE resin. These results indicated that amine groups have taken part in the nitrate adsorption process, and the adsorption mechanism included the ion exchange by the displacement of Cl^- with nitrate ions.

3.1.4. Raman spectra analysis

Fig. 4 shows the Raman spectra of ALR-AE resin, nitrate solution and nitrate-loaded ALR-AE resin. In the Raman spectrum of ALR-AE resin, appearance of peaks at 2974.7, 1456.7 and 1607.3 cm^{-1} was the characteristic peaks of cellulose and hemicellulose chains. Nitrate in a 0.5 mol/L of nitrate solution had a characteristic peak at 1048 cm^{-1} [25]. After the adsorption process, the nitrate on ALR-AE resin showed its Raman peak at 1044.3 cm^{-1}, which was similar to the reported data in our previous work for the adsorption of nitrate onto amine-crosslinked wheat straw [25]. The similar band position of the soluble and adsorbed nitrate showed no strong chemical interaction between the adsorbed nitrate and ALR-AE resin, and nitrate ions still existed on surface of ALR-AE resin in ionic form. This result validated the ion exchange mechanism for the removal of nitrate by ALR-AE resin [31].

3.2. Adsorption tests

3.2.1. Effect of contact time and pH on adsorption of nitrate by ALR-AE resin

Fig. 5 shows the effect of contact time on the adsorption of nitrate by ALR-AE resin at different pH (2.0, 4.0, 6.0, 9.0, 12.0). For all the pH, three distinct adsorption stages were observed before the equilibrium stage. Stage 1 (1–5 min), represented by a steep slope, reflected a rapid adsorption rate with uptake of 80–85% of nitrate. The extremely rapid adsorption process corresponded to the instantaneous monolayer adsorption of nitrate on the surface of ALR-AE resin [32,33]. Stage 2 (5–10 min), signified by a gentle slope, was characterized by a gradually reduced adsorption rate prior to reaching equilibrium. The decreased adsorption rate in stage 2 reflected a more thorough utilization of adsorption sites on ALR-AE resin. Stage 3 (after 10 min), the system reached an equilibrium state.

Fig. 5 also shows the effect of pH value on the adsorption capacity of ALR-AE resin for nitrate. It showed a gentle increased trend in the nitrate adsorption capacity as the pH increased from 2.0 to 9.0. The adsorption capacity significantly decreased with the further increase in pH from 9.0 to 12.0. At alkaline condition, the repulsive electrostatic interaction between the surface of ALR-AE resin and nitrate ions would be enhanced, resulting from the increased negatively charged surface sites. In addition to this, the presence of excess OH^- ions at higher pH value would compete with the nitrate for the adsorption sites on ALR-AE resin and a result of the adsorption capacity for nitrate decreased.

Equilibrium pH values were examined after the uptake of nitrate by ALR-AE resin at different initial pH (figure was not given). The equilibrium pH values after the adsorption experiments (initial pH 2.0, 4.0, 6.0, 9.0 and 12.0) were 2.3, 4.6, 6.2, 6.9, and 11.1, respectively. It showed that the equilibrium pH decreased significantly when the initial pH values were in range of 9.0–12.0. This could be attributed to the weakly acidic hydroxyl and carboxyl inherently in ALR-AE resin, which decreased the pH of solutions in mild alkali conditions.

3.2.2. Adsorption isotherm

Temperature is an important parameter for the adsorption process. Fig. 6 illustrates the effect of temperature (293, 303, 313 and 323 K) on the adsorption of nitrate by ALR-AE resin. The adsorption capacity of ALR-AE resin for nitrate decreased with the increase in temperature, illustrating an exothermic nature for the adsorption process [34]. The adsorption results were analyzed by the

Table 3
Isotherm parameters for adsorption nitrate by ALR-AE resin.

Temperature (K)	Langmuir			Freundlich		
	Q_{max} (mg/g)	b (l/mg)	R^2	K_F (mg/g)/(mg/l)	n	R^2
293	44.61	0.045	0.992	7.87	2.49	0.985
303	43.64	0.044	0.992	7.30	2.40	0.976
313	42.89	0.040	0.993	7.35	2.42	0.982
323	40.54	0.038	0.994	7.29	2.39	0.979

Table 4
Q_{max} of NO_3^- in different adsorbents.

Adsorbents/resins	Q_{max} (mg/g)	References
ALR-AE resin	40.54–44.61	This work
Activated carbon	5.8	[35]
Commercial anion exchange resins	36.0–71.6	[35,36]
Amberlite IRA 400	65.36	[37]
Actived sepiolite	9.8	[38]
Amberlite IRA 400	87.4	[39]

Langmuir and Freundlich isotherm models equations, and the data were shown in Table 3.

Langmuir equation:

$$\frac{1}{q_e} = \frac{1}{Q_{max}} + \frac{1}{bQ_{max}}\frac{1}{C_e} \quad (1)$$

Reundlich equation:

$$\ln\ q_e = \ln K_F + \frac{1}{n}\ln C_e \quad (2)$$

where C_e, the equilibrium concentration in solution (mg/L); Q_{max}, the monolayer capacity of ALR-AE resin (mg/g); b, the Langmuir constant (L/mol) and related to the free energy of adsorption; K_F, the Freundlich constant (L/g); n (dimensionless), the heterogeneity factor.

Results shown in Table 3 indicated that Langmuir isotherm generated the better agreement with experimental data for adsorption systems in comparison with Freundlich isotherm. The Q_{max} for nitrate at ambient temperature condition (293 K) was 44.61 mg/g. Table 4 shows the comparison of the Q_{max} of various adsorbents/resins for nitrate. Experimental data shown in Table 4 indicated that the ALR-AE resin was excellent in the adsorption of nitrate, and can be in competition with some commercially available adsorbents; this provided strong evidence of the potential of ALR-AE resin for the technological applications of nutrient substances removal from aqueous solutions.

3.2.3. Column adsorption

When the sorption zone moved up and the upper edge of this zone reached the bottom of the column, the effluent concentration started to rise rapidly. This was called the breakthrough point. The desired breakthrough point was determined to be $0.1C_t/C_0$. The point where the effluent concentration reached 95% ($C_t/C_0 = 0.95$) of its influent value was called the point of column exhaustion.

The results in Fig. 7 presented the nitrate adsorption curves with different mass of ALR-AE resin in column (0.5, 1.0 and 2.0 g). As was shown in Fig. 7, when the mass of ALR-AE resin were 0.5, 1.0 and 2.0 g, the breakthrough points occurred at the breakthrough volumes of 120, 250 and 490 mL, respectively. As the nitrate solution continued to flow into the column, the ALR-AE resin gradually became saturated with nitrate ions and became less effective for further adsorption. The points on the S-shaped curves at which the nitrate concentrations approached their exhaustion values were about 500, 700 and 1100 mL for mass of 0.5, 1.0 and 2.0 g, respectively. The saturated adsorption capacities of ALR-AE resin (0.5, 1.0 and 2.0 g) in column were about 37.5, 37.9 and 38.9 mg/g, which accounted for about 84.1%, 85.0% and 87.2% of the resin's Q_{max}.

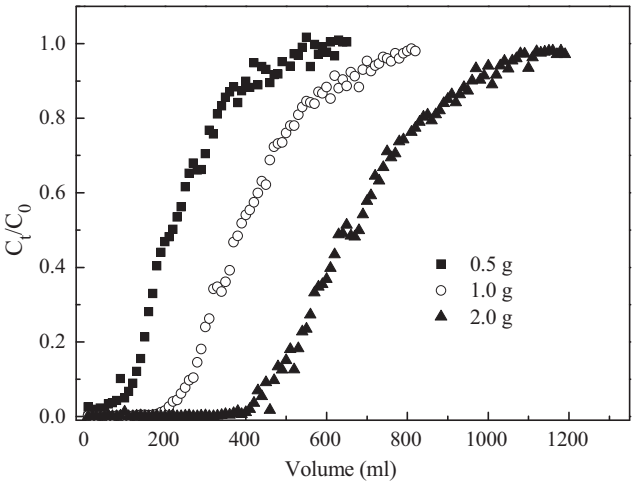

Fig. 7. Effect of mass of ALR-AE resin on the breakthrough curves (influent concentration: 100 mg/L, flow rate: 5 mL/min).

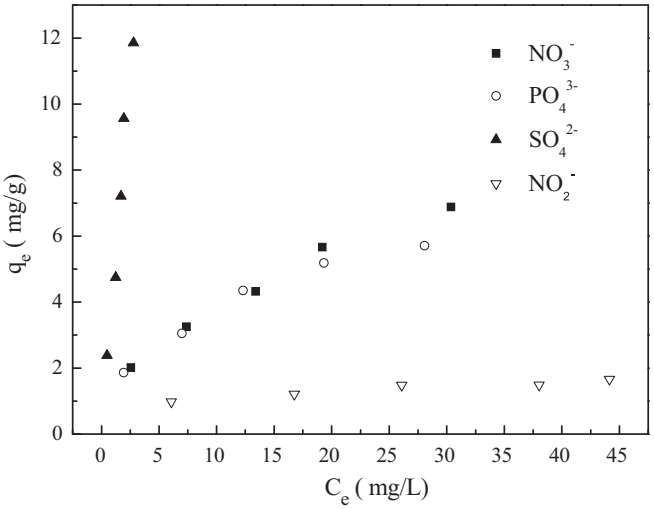

Fig. 8. Competition adsorption of different ions onto ALR-AE resin.

These results indicated that the efficiency of the adsorption sites on ALR-AE resin would be enhanced with more ALR-AE resin packed in column.

3.2.4. Competitive adsorption

Till now all the adsorption results discussed above were obtained taking nitrate ion only. However, in reality the nitrate contaminated water contains several other coexisting anions which can equally compete for the adsorption sites in the adsorption process. In order to see effect of interfering ions on adsorption of nitrate, a mixture of commonly coexisting anions in water, such as, SO_4^{2-}, PO_4^{3-} and NO_2^- ions were added to nitrate solutions.

Fig. 8 shows the competitive behavior of the NO_3^-, SO_4^{2-}, PO_4^{3-} and NO_2^- ions for adsorption sites on ALR-AE resin. In

Table 5
Water qualities of three actual water samples.

No.		pH	NO_3^- (mg/L)	NO_2^- (mg/L)	PO_4^{3-} (mg/L)	SO_4^{2-} (mg/L)	AsO_2^- (mg/L)
1#	Original water	8.3	4.49	0.36	0.16	5	–
	After adsorption[a]	6.2	0.1	0.02	N/A	0.03	–
2#	Original water	8.7	36.5	11.32	6.96	75.7	–
	After adsorption[a]	6.4	10.9	5.8	0.34	5.8	–
3#	Original water	8.1	21.5	–	3.3	54.6	1.24
	After adsorption[a]	6.1	2.4	–	0.12	1.2	0.21

[a] Dosage of ALR-AE resin: 2 g/L.

the case of nitrate, the adsorbed amount decreased significantly in the presence of SO_4^{2-}, PO_4^{3-} and NO_2^-. The preferential adsorption capacity of the ALR-AE resin followed the order as: $SO_4^{2-} > NO_3^- \approx PO_4^{3-} > NO_2^-$. It was observed that the ALR-AE resin showed its specialistic adsorption property for SO_4^{2-} ions, with the adsorbed amount several times higher than those of other anions. It was also evident from the figure that the percentage removal of nitrate by ALR-AE resin was similar to that of phosphate. So nitrate removal by ALR-AE resin might face some difficulties if the concentrations of coexisting anions in the water were high.

3.2.5. Utilization of the resin in actual water samples

To validate the applicability of the ALR-AE resin in practical utilization, three actual water samples were pertinently selected from Longhu Mountain reservoir (1#), effluent from the wastewater treatment plant (2#) and Yihe river (3#). The removal efficiencies of ALR-AE resin for these samples were shown in Table 5. Although the water qualities of these samples varied each other, results in Table 5 indicated that almost all the anions could be removed from these water samples. This indicated that the ALR-AE resin could be used for the treatment of many ionic polluted wastewaters. The water in Yihe River (3#) was polluted by arsenite anion. A special result was observed in 3# water sample, which showed an uptake of arsenite anion (from 1.24 mg/L to 0.21 mg/L) from water. This result replenished the applicability of ALR-AE resin for the removal of some toxic anions in practical utilization.

4. Conclusion

The ALR-AE resin used in this work was prepared by the amination reaction. Large amounts of amine groups were detected in structure of the ALR-AE resin. The adsorption properties of the ALR-AE resin for nitrate were determined by the static and dynamic adsorption tests. The maximum adsorption capacity (Q_{max}) for nitrate was 45.61 mg/g. The adsorption data showed an exothermic nature for the adsorption of nitrate by ALR-AE resin, and the equilibrium time for the adsorption process was about 10 min. The competitive adsorption property (NO_3^-, SO_4^{2-}, PO_4^{3-} and NO_2^-) was discussed, and the preferential adsorption capacity of the ALR-AE resin followed the order as: $SO_4^{2-} > NO_3^- \approx PO_4^{3-} > NO_2^-$. Three actual water samples were selected and ALR-AE resin showed its removal capacity for almost all anions including the arsenite anions from water.

Acknowledgments

The research was supported by the National Natural Science Foundation of China (50878121), National Natural Science Foundation of China (51178252), Shandong Outstanding Young and Middle-aged Scientists Research Award Fund (BS2011HZ007), Key Projects in the National Science & Technology Pillar Program in the Eleventh Five-year Plan Period (2006BAJ08B05-2) and National Major Special Technological Programmes Concerning Water Pollution Control and Management in the Eleventh Five-year Plan Period (2008ZX07010-008).

References

[1] Y.L. Wang, C.S. Zhao, Y.X. Liu, P.Y. Qin, F. Yang, P. You, Study on pulping of Lu-bamboo, Hunan Papermaking 3 (2002) 12–14.
[2] Y.Y. Zhou, Ozone bleaching of arundinaceous ethanol pulp, China Pulp. Paper Ind. 31 (2010) 82–85.
[3] A.A. Shatalov, H. Pereira, Kinetics of organosolv delignification of fibre crop *Arundo donax* L., Ind. Crops Prod. 21 (2005) 203–210.
[4] R.E. Perdue, *Arundo donax*—source of musical reeds and industrial cellulose, Econ. Bot. 12 (1958) 368–404.
[5] C.D. Dalianis, Ch A. Sooter, M.G. Christou, Growth, biomass productivity and energy potential of giant reed (*Arundo donax*) and elephant grass (*Miscanthus sinensis giganteus*), in: Ph. Chartier, A.A.C.M. Beenackers, G. Grassi (Eds.), Proceedings of the Eighth European Biomass Conference, Vienna, Pergamon, UK, 1994, pp. 575–582.
[6] C. Dora, M. Gisela, A. Gutierrez, J.D. Silvestre Armando, C. del Rio Jose, Chemical characterization of the lipophilic fraction of giant reed (*Arundo donax*) fibres used for pulp and paper manufacturing, Ind. Crops Prod. 26 (2007) 229–236.
[7] A.A. Shatalov, H. Pereira, *Arundo donax* L. reed: new perspectives for pulping and bleaching. 5. Ozone-based TCF bleaching of organosolv pulps, Bioresour. Technol. 99 (2008) 472–478.
[8] A.A. Shatalov, T. Quilhó, H. Pereira, *Arundo donax* L. reed: new perspectives for pulping and bleaching. Part 1. Raw material characterization, TAPPI J. 84 (2001) 96–107.
[9] A.A. Shatalov, H. Pereira, *Arundo donax* L. reed: new perspectives for pulping and bleaching. Part 2. Organosolv delignification, TAPPI J. 84 (2001) 1–12.
[10] A.A. Shatalov, H. Pereira, Carbohydrate behaviour of *Arundo donax* L. in ethanol–alkali medium of variable composition during organosolv delignification, Carbohydr. Polym. 49 (2002) 331–336.
[11] A.A. Shatalov, H. Pereira, *Arundo donax* L. reed: new perspectives for pulping and bleaching. Part 4. Peroxide bleaching of organosolv pulps, Bioresour. Technol. 96 (2005) 865–872.
[12] W.Y. Wang, Q.Y. Yue, X. Xu, B.Y. Gao, J. Zhang, Q. Li, J.T. Xu, Optimized conditions in preparation of giant reed quaternary amino anion exchanger for phosphate removal, Chem. Eng. J. 157 (2010) 161–167.
[13] J. Zhang, Y. Li, C. Zhang, Y. Jing, Adsorption of malachite green from aqueous solution onto carbon prepared from *Arundo donax* root, J. Hazard. Mater. 150 (2008) 774–782.
[14] X.L. Pan, D.Y. Zhang, Removal of malachite green from water by Firmiana simplex wood fiber, Electron. J. Biotechnol. 12 (2009) 1–10.
[15] J.P. de Celis, M.S. Villaverde, A.L. Cukierman, N.E. Amadeo, Oxidative dehydrogenation of ethylbenzene to styrene on activated carbons derived from a native wood as catalyst, Lat. Am. Appl. Res. 39 (2008) 165–171.
[16] H. Liu, J. Zhang, Removal of cephalexin from aqueous solutions by original and Cu (II)/Fe (III) impregnated activated carbons developed from lotus stems: Kinetics and equilibrium studies, J. Hazard. Mater. 185 (2011) 1528–1535.
[17] L. Ren, J. Zhang, Preparation and evaluation of cattail fiber based activated carbon for 2,4-dichlorophenol and 2,4,6-trichlorophenol removal, Chem. Eng. J. 168 (2011) 553–561.
[18] W.F. Liu, J. Zhang, Sorption of norfloxacin by lotus stalk-based activated carbon and iron-doped activated alumina: Mechanisms, isotherms and kinetics, Chem. Eng. J. 117 (2011) 431–438.
[19] E.C.H.E.T. Lucassen, A.J.P. Smolders, A.L. Van Der Salm, J.G.M. Roelofs, High groundwater nitrate concentrations inhibit eutrophication of sulphate-rich freshwater wetland, Biogeochemistry 67 (2004) 249–267.
[20] S. Marlene, V. Micaela, V. Vitor, Effects of nitrate reduction on the eutrophication of an urban man-made lake (Palácio de Cristal, Porto, Portugal), Environ. Technol. 32 (2011) 1009–1015.
[21] J.A. Camargo, Á. Alonso, Ecological and toxicological effects of inorganic nitrogen pollution in aquatic ecosystems: a global assessment, Environ. Int. 32 (2006) 831–849.
[22] X. Xu, B.Y. Gao, X. Tang, Q.Y. Yue, Q.Q. Zhong, Q. Li, Characteristics of cellulosic amine-crosslinked copolymer and its sorption properties for Cr(VI) from aqueous solutions, J. Hazard. Mater. 189 (2011) 420–426.

[23] V. Murphy, H. Hughes, P. McLoughlin, Comparative study of chromium biosorption by red, green and brown seaweed biomass, Chemosphere 70 (2008) 1128–1134.
[24] I.H. Yoon, X. Meng, C. Wang, K.W. Kim, S. Bang, E. Choe, L. Lippincott, Perchlorate adsorption and desorption on activated carbon and anion exchange resin, J. Hazard. Mater. 164 (2009) 87–94.
[25] X. Xu, B.Y. Gao, Q.Q. Zhong, Q.Y. Yue, Q. Li, Sorption of nitrate onto amine-crosslinked wheat straw: characteristics, column sorption and desorption properties, J. Hazard. Mater. 186 (2011) 206–211.
[26] S.H. Chen, Q.Y. Yue, B.Y. Gao, Q. Li, X. Xu, Preparation and characteristics of anion exchanger from corn stalks, Desalination 274 (2011) 113–119.
[27] Y. Wang, B.Y. Gao, W.W. Yue, Q.Y. Yue, Adsorption kinetics of nitrate from aqueous solutions onto modified wheat residue, Colloids Surf., A 308 (2007) 1–5.
[28] Q.Y. Yue, W.Y. Wang, B.Y. Gao, X. Xu, J. Zhang, Q. Li, Phosphate removal from aqueous solution by adsorption on modified giant reed, Water Environ. Res. 82 (2010) 374–381.
[29] M. Iqbal, A. Saeed, S.I. Zafar, FTIR spectrophotometry, kinetics and adsorption isotherms modeling, ion exchange, and EDX analysis for understanding the mechanism of Cd^{2+} and Pb^{2+} removal by mango peel waste, J. Hazard. Mater. 164 (2009) 61–171.
[30] M.A. Wahab, S. Jellali, N. Jedidi, Ammonium biosorption onto sawdust: FTIR analysis, kinetics and adsorption isotherms modeling, Bioresour. Technol. 101 (2010) 5070–5075.
[31] S. Baidas, B.Y. Gao, X.G. Meng, Perchlorate removal by quaternary amine modified reed, J. Hazard. Mater. 189 (2011) 54–61.
[32] A.M. Díez-Pascual, A. Compostizo, A. Crespo-Colín, R.G. Rubio, R. Miller, Adsorption of water-soluble polymers with surfactant character: adsorption kinetics and equilibrium properties, J. Colloid Interface Sci. 307 (2007) 398–404.
[33] A.A.M. Daifullah, B.S. Girgis, Impact of surface characteristics of activated carbon on adsorption of BTEX, Colloids Surf., A 214 (2003) 181–193.
[34] E.A. Ferreiro, S.G. de Bussetti, Thermodynamic parameters of adsorption of 1,10-phenanthroline and 2,2′-bipyridyl on hematite, kaolinite and montmorillonites, Colloids Surf., A 301 (2007) 117–128.
[35] H.J. Park, C.K. Na, Preparation of anion exchanger by amination of acrylic acid grafted polypropylene nonwoven fiber and its ion-exchange property, J. Colloid Interface Sci. 301 (2006) 46–54.
[36] U.S. Orlando, A.U. Baes, W. Nishijima, Preparation of agricultural residue anion exchangers and its nitrate maximum adsorption capacity, Chemosphere 48 (2002) 1041–1046.
[37] M. Chabani, A. Amrane, A. Bensmaili, Kinetics of nitrates adsorption on Amberlite IRA 400 resin, Desalination 206 (2007) 560–567.
[38] N. Öztürk, T.E. Bektaş, Nitrate removal from aqueous solution by adsorption onto various materials, J. Hazard. Mater. B112 (2004) 155–162.
[39] J. Beltran-Heredia, J.R. Dominguez, Y. Cano, I. Jimenez, Nitrate removal from groundwater using Amberlite IRN-78: modelling the system, Appl. Surf. Sci. 252 (2006) 6031–6035.